ELSEVIER

Journal of Applied Geophysics 49 (2002) 231–244

Journal of Applied Geophysics

www.elsevier.com/locate/jappgeo

Analytic signal approach and its applicability in environmental magnetic investigations

Ahmed Salem [a,*], Dhananjay Ravat [b], T. Jeffrey Gamey [c], Keisuke Ushijima [a]

[a]Department of Earth Resources Engineering, Faculty of Engineering, Kyushu University 6-10-1, Higashi-ku, Fukuoka 812-8581, Japan
[b]Department of Geology MS 4234, Southern Illinois University at Carbondale, Carbondale, IL 62901, USA
[c]Oak Ridge National Laboratory, Oak Ridge, TN 37831-6038, USA

Received 27 April 2001; accepted 18 January 2002

Abstract

We investigate the analytic signal method and its applicability in obtaining source locations of compact environmental magnetic objects. Previous investigations have shown that, for two-dimensional magnetic sources, the shape and location of the maxima of the amplitude of the analytic signal (AAS) are independent of the magnetization direction. In this study, we show that the shape of the AAS over magnetic dipole or sphere source is dependent on the direction of magnetization and, consequently, the maxima of the AAS are not always located directly over the dipolar sources. Maximum shift in the horizontal location is obtained for magnetic inclination of 30°. The shifts of the maxima are a function of the source-to-observation distance and they can be up to 30% of the distance. We also present a method of estimating the depths of compact magnetic objects based on the ratio of the AAS of the magnetic anomaly to the AAS of the vertical gradient of the magnetic anomaly. The estimated depths are independent of the magnetization direction. With the help of magnetic anomalies over environmental targets of buried steel drums, we show that the depths can be reliably estimated in most cases. Therefore, the analytic signal approach can be useful in estimating source locations of compact magnetic objects. However, horizontal locations of the targets derived from the maximum values of the AAS must be verified using other techniques. © 2002 Elsevier Science B.V. All rights reserved.

Keywords: Magnetic; Analytic signal; Depth estimation; Environmental

1. Introduction

A large amount of environmentally hazardous material has been laid around the world, sometimes killing innocent people. Since these materials are often buried in ferrometallic containers, detection and precise location of such objects are becoming increasingly important in environmental investigations worldwide.

The magnetic method is one of the best geophysical techniques for locating and mapping the distribution of ferrometallic objects. Recent development of airborne magnetic systems (Gamey and Mahler, 1999; Gamey et al., 2000) has made it possible to rapidly detect much smaller objects using airborne magnetic surveys than it was possible before. However, airborne magnetic measurements create large volumes of data that need to be analyzed and interpreted, and this can be time consuming. Thus, there is a need for an automatic method of interpretation.

Since the 1970s, a variety of semiautomatic methods, based on the use of gradients (derivatives) of the

* Corresponding author.
E-mail address: Salem@mine.kyushu-u.ac.jp (A. Salem).

PII: S0926-9851(02)00125-8

magnetic field anomalies, have been developed for the determination of geometric parameters such as locations of boundaries and depths of the causative sources. As faster computers and commercial software have become widely available, these techniques are being used more extensively. One of these techniques is the approach of the analytic signal of magnetic anomalies, which was initially used in its complex function form and makes use of the properties of Hilbert transform (Nabighian, 1972; Atchuta Rao et al., 1981; Nelson, 1988; Pederson, 1989; Blakely, 1995).

The amplitude of the analytic signal (AAS) is defined as the square root of the squared sum of the vertical and two orthogonal horizontal derivatives of the magnetic field, where the horizontal and vertical derivatives of the magnetic field are Hilbert transform pairs (Debeglia and Corpel, 1997) over 2D sources. It had been used successfully in the form of profile data to locate dyke bodies (Nabighian, 1972, 1974, 1984; Atchuta Rao et al., 1981). Moreover, the approach was further developed by Roest et al. (1992) for the interpretation of aeromagnetic maps (see also MacLeod et al., 1993). The improvements of the approach in the interpretation of aeromagnetic data were presented by Hsu et al. (1996, 1998) and Debeglia and Corpel (1997). Furthermore, Thurston and Smith (1997) presented a variation of the approach (also known as local wave number).

The AAS of magnetic anomalies can be easily computed. The horizontal derivatives can be calculated directly from a total field grid using a simple 3×3 difference filter. Also, both the horizontal and vertical gradients can be calculated in the frequency domain using the conventional Fast Fourier Transform (FFT) techniques. Another reason for the appeal of the method is that the locations and depths of the sources are found with only a few assumptions about the nature of the source bodies, which usually are assumed as 2D magnetic sources (for example, step, contact, horizontal cylinder, or dyke). For these geological models, the shape of the amplitude of the analytic signal is a bell-shaped symmetric function located directly above the source body. In addition, depths can be obtained from the width of the AAS.

Despite the above advances, only a limited amount of work has been published on the practical use of the analytic signal approach in environmental magnetic applications. In these applications, the approach was only used as a presentation of magnetic anomalies in place of usual total field maps (see, for example, Pawlowski et al., 1995; Gamey et al., 1997, 2000). In this paper, we investigate the analytic signal approach from the point of its theoretical limitations and practical utility in the field of the detection of compact magnetic sources. First, we define the analytic signal equation for dipolar sources. Then, the analytic signal responses from theoretical examples and field data of steel drums are investigated with regard to their source locations. Although the results show that the approach does not usually give accurate horizontal locations, we have developed a method that can provide a good estimate of the depth of compact magnetic sources.

2. Analytic signal of a dipole source

In Cartesian coordinates, the elements of the magnetic field (B_x, B_y, and B_z) caused by a dipole source (Blakely, 1995) can be written as

$$B_x = K\frac{(3Dr_x - r^2 l)}{r^5}, \tag{1}$$

$$B_y = K\frac{(3Dr_y - r^2 m)}{r^5}, \text{ and} \tag{2}$$

$$B_z = K\frac{(3Dr_z - r^2 n)}{r^5}, \tag{3}$$

where K is the dipole moment, $r=(r_x{}^2+r_y{}^2+r_z{}^2)^{1/2}$ is the vector distance directed from the dipole to the observation point, r_x, r_y, and r_z are the components of r in x, y, and z directions, and l, m, n, and D are quantities related to the magnetization direction of the dipole source. If a is the inclination and b is the angle between the horizontal component and the geographic north (magnetic declination), the quantities representing the magnetization direction are described as follows:

$$\left.\begin{aligned} l &= \cos(a)\cos(b) \\ m &= \cos(a)\sin(b) \\ n &= \sin(a) \\ D &= lr_x + mr_y + nr_z \end{aligned}\right\}. \tag{4}$$

Also, we have

$$\Delta T = LB_x + MB_y + NB_z, \tag{5}$$

where ΔT is the total field magnetic anomaly produced by a dipole source, $L = \cos(A)\ \cos(B)$, $M = \cos(A)\ \sin(B)$, $N = \sin(A)$, where A is the inclination of the normal geomagnetic field and B is the angle between the horizontal component of the geomagnetic field vector and the x-axis (the geographic north). For simplicity of derivation, we assume that the magnetic declination is zero and the magnetization is induced only. Thus, $a = A$ and $b = B$. Then, from Eq. (5), we get

$$\Delta T = K\frac{(3D^2 - r^2)}{r^5}. \tag{6}$$

The gradients of ΔT with respect to the variables x, y, and z are as follows:

$$\frac{\partial T}{\partial x} = 3K\frac{(2r^2Dl - 5D^2r_x + r^2r_x)}{r^7}, \tag{7}$$

$$\frac{\partial T}{\partial y} = 3K\frac{(2r^2Dm - 5D^2r_y + r^2r_y)}{r^7}, \text{ and} \tag{8}$$

$$\frac{\partial T}{\partial z} = 3K\frac{(2r^2Dn - 5D^2r_z + r^2r_z)}{r^7}. \tag{9}$$

The 3D amplitude of the analytic signal expression (Roest et al., 1992) is given by

$$|\mathrm{AAS}(x,y)| = \sqrt{\left(\frac{\partial T}{\partial x}\right)^2 + \left(\frac{\partial T}{\partial y}\right)^2 + \left(\frac{\partial T}{\partial z}\right)^2}. \tag{10}$$

Thus, the AAS over a dipole source can be defined by substituting Eqs. (7)–(9) in Eq. (10) as

$$|\mathrm{AAS}(x,y)| = 3K\sqrt{\frac{5D^4 - 2r^2D^2 + r^4}{r^{12}}}. \tag{11}$$

In the above expression, the term D is not symmetric about the source location. As a result, the overall characteristic shape of the AAS over dipolar sources is dependent on the magnetization direction. Linping et al. (1997), in their comments to Qin (1994), also showed that the analytic signal of 3D sources is dependent on the inclination of magnetization direction and that it does not always produce symmetrical anomalies.

To understand the effect of the magnetization direction on the analytic signal response of dipolar sources and to judge the applicability of the approach to provide horizontal locations for such objects, we simulated a set of analytic signal responses for magnetic dipole sources with different magnetization directions. In our coordinate system, positive x-direction is magnetic north and positive y-direction is magnetic east. A dipole source has a magnetic moment of 10 A m^2 and is placed at a horizontal location of $x = 10$ m and $y = 10$ m and at a depth of 3 m from the origin of the coordinate system. A magnetic declination of 0° with different magnetic inclinations (0°, 30°, 60°, and 90°) was assigned to the dipole source. Then, for each magnetization direction, the analytic signal response was computed on a square grid of 20 × 20 m at a grid spacing of 1 m using Eq. (11).

Fig. 1a,b shows the normalized AAS response for the dipole source for each of the above magnetization directions along two profiles (north–south and east–

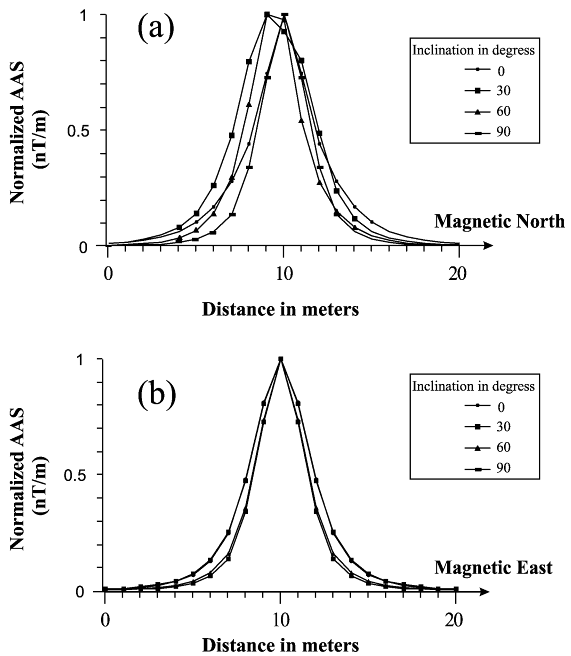

Fig. 1. A normalized amplitude of the analytic signal response of a dipole with different inclinations: (a) along the magnetic north–south direction; (b) along the east–west direction.

west, respectively). It is clear that the shape of the AAS is dependent on the magnetization direction, especially in the north–south direction (direction of the horizontal component of the dipole). This dependency leads to a certain amount of asymmetry in the case of oblique magnetic inclination, which is large enough to cause inaccuracies in the estimated horizontal location of the source based on the maxima of the AAS. However, in the east direction (perpendicular to the horizontal component of the dipole), the shape of the AAS appears to be symmetric (Fig. 1b).

We have further analyzed quantitatively the location errors resulting from using the maximum of the AAS as an indication of horizontal location of compact magnetic sources. We simulated analytic signal signatures of dipole sources with varying magnetic directions and depths. Dipole sources of the same magnetic moment were placed at the same horizontal location but buried at different depths ranging from 1 to 10 m with a 1-m interval. At each depth, we computed the AAS for a set of magnetic inclinations and declinations varying from 0° to 90° at an interval of 10°. We found that the location of the maximum of the AAS depends on both the magnetic inclination and depth of the source. The direction of the magnetic declination appears to guide the direction of the shift of the maximum. For the induced cases, the maxima are shifted in the direction opposite to the magnetic north.

To show the amount of location errors, we present the case of magnetic declination of 0° as an example; the results for other declinations are the same. Fig. 2 shows the horizontal location errors for each magnetic inclination and depth. Generally, for near vertical or horizontal fields, the horizontal location error is very small and it is maximum at the magnetic inclination of 30°. For the worst case, the error represents approximately 30% of the depth. Thus, for sources that are located at a depth of 6 m, an error of 2 m may be expected in the horizontal location. These horizontal location errors are acceptable for certain environmental situations such as very shallow or large objects. In other applications, care should be taken when interpreting dipolar sources using the analytic signal approach. For example, in regional aeromagnetic applications, horizontal locations can be in error by up to 3 km for dipolar sources located at depths in the range of 10 km. In the case of Magsat satellite magnetic data (400 km altitude), dipole-like sources that are located within the Earth's crust may be detected at mid-latitude with an error of about 130 km in the horizontal location.

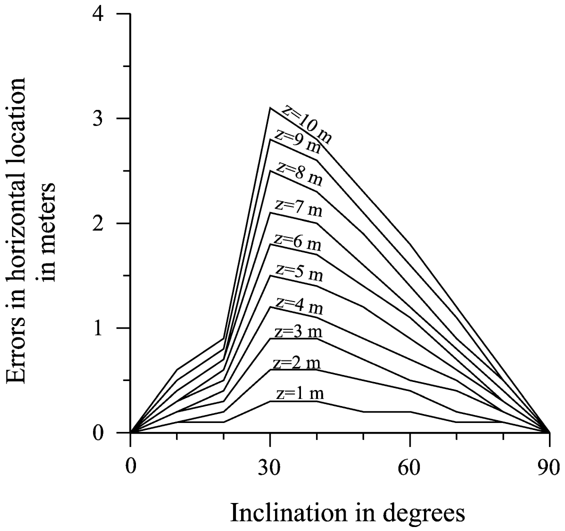

Fig. 2. Errors resulting from choosing the horizontal location based on the maximum value of the analytic signal.

3. Estimating depth of compact magnetic sources

Because of the asymmetric and unequal half-width nature of the shape of the AAS at different latitudes (with respect to the true source location), there is no single relationship to estimate depths of dipolar sources from the shapes of their analytic signals as in case of 2D magnetic sources (see, for example, MacLeod et al., 1993). However, we have developed a method in which depths of compact magnetic sources are estimated from the ratio of the analytic signal to the higher order analytic signal in an approach similar to the one used by Hsu et al. (1996, 1998) for 2D magnetic sources.

The amplitude of the nth order derivative $\mathrm{AAS}_n(x,y)$ can be expressed equally in terms of either the vertical or horizontal derivatives (Debeglia and Corpel, 1997), respectively, as

$$|\mathrm{AAS}_n(x,y)| = \sqrt{\left(\frac{\partial T_n^z}{\partial x}\right)^2+\left(\frac{\partial T_n^z}{\partial y}\right)^2+\left(\frac{\partial T_n^z}{\partial z}\right)^2} \text{ and} \tag{12a}$$

$$|\mathrm{AAS}_n(x,y)| = \sqrt{\left(\frac{\partial T_n^h}{\partial x}\right)^2 + \left(\frac{\partial T_n^h}{\partial y}\right)^2 + \left(\frac{\partial T_n^h}{\partial z}\right)^2}. \tag{12b}$$

It may be preferable to use Eq. (12a) because the vertical derivatives better resolve depths rather than the horizontal derivatives. Accordingly, the first-order analytic signal (AAS_1) can be written as

$$|\mathrm{AAS}_1(x,y)| = \sqrt{\left(\frac{\partial T_1^z}{\partial x}\right)^2 + \left(\frac{\partial T_1^z}{\partial y}\right)^2 + \left(\frac{\partial T_1^z}{\partial z}\right)^2}, \tag{13}$$

where $(\partial T_1{}^z)/(\partial x)$, $(\partial T_1{}^z)/(\partial y)$, and $(\partial T_1{}^z)/(\partial z)$ are the first derivatives of the vertical gradient. If the dipole source is located at a depth z_d from the measuring plan ($z=0$), at the measuring point above the dipole source ($r_x=0$ and $r_y=0$), we can define these derivatives as

$$\left(\frac{\partial T_1^z}{\partial x}\right)_{r_x=0,r_y=0} = \frac{-24Knl}{z_\mathrm{d}^5},$$

$$\left(\frac{\partial T_1^z}{\partial y}\right)_{r_x=0,r_y=0} = \frac{-24Knm}{z_\mathrm{d}^5}, \text{ and} \tag{14}$$

$$\left(\frac{\partial T_1^z}{\partial z}\right)_{r_x=0,r_y=0} = \frac{12K(3n^2-1)}{z_\mathrm{d}^5}.$$

By substituting Eq. (14) in Eq. (13), we obtain the value of the AAS_1 directly above the source as

$$|\mathrm{AAS}_1|_{r_x=0,r_y=0} = 12K\frac{\sqrt{5n^4-2n^2+1}}{z_\mathrm{d}^5}. \tag{15}$$

Similarly, the value of the AAS_0 above the source can be defined from Eq. (11) as

$$|\mathrm{AAS}_0|_{r_x=0,r_y=0} = 3K\frac{\sqrt{5n^4-2n^2+1}}{z_\mathrm{d}^4}. \tag{16}$$

Therefore, the depth z_d can be obtained from Eqs. (15) and (16) as

$$z_\mathrm{d} = 4\frac{|\mathrm{AAS}_0|_{r_x=0,r_y=0}}{|\mathrm{AAS}_1|_{r_x=0,r_y=0}}. \tag{17}$$

Eq. (17) shows that the depth can be obtained from the ratio of the analytic signals ($\mathrm{AAS}_0/\mathrm{AAS}_1$) at a point directly above the dipolar source. Note that the estimation of the depth in this case is completely independent of the magnetization direction of the dipole source.

To demonstrate the feasibility of this relation, we present two synthetic examples for induced dipole sources at different depths. In the two examples, the induced magnetic field is the same and has an inclination of 30° and a declination of 20°. The dipole sources are placed at the same horizontal location ($x=10$ m and $y=10$ m from the origin) and have the same magnetic moment of 10 A m^2. In the first example, the dipole source is placed at a depth of 3 m and in the second example, it is placed at a depth of 5 m. Fig. 3a,b shows the total field magnetic anomaly maps over the two sources. The requisite derivatives to form AAS_0 and AAS_1 were computed in the frequency domain. The ratio of these analytic signal signatures multiplied by factor 4 was calculated and is illustrated in Fig. 3c,d. It is clear that the analytic signal ratio can provide an accurate estimate of the depth at the horizontal location of the sources ($x=10$ m and $y=10$ m). The estimated depths are 3.06 m for the first example and 4.96 m for the second one. It can also be seen that the change in the analytic signal ratio is small near the horizontal location of the source. Therefore, even though the maxima of the AAS_0 may not exactly locate the horizontal locations of the sources, the depths determined from the ratio of the maxima in AAS_0 to AAS_1 would still be correct.

To better understand the errors in depths calculated at the locations of the maximum of the AAS_0, we performed a study for dipole sources at the same horizontal locations as above but at varying depths, starting from 1 to 10 m with a small interval of 0.1 m. Magnetic inclination of 30° was assigned to the dipole sources, as this inclination gives the maximum shift in the horizontal locations (Fig. 2). Then, depths were calculated using Eq. (17) at the locations of maxima AAS_0 and compared with actual depths. We found that the maximum percentage error in the depth estimate did not exceed 8%. This implies that the method can provide a good depth estimate even when the calculation is made at the locations of the maxima of the AAS_0. This attribute is especially important because the location of maximum of AAS_0 may not exactly coincide with the location of the maximum AAS_1.

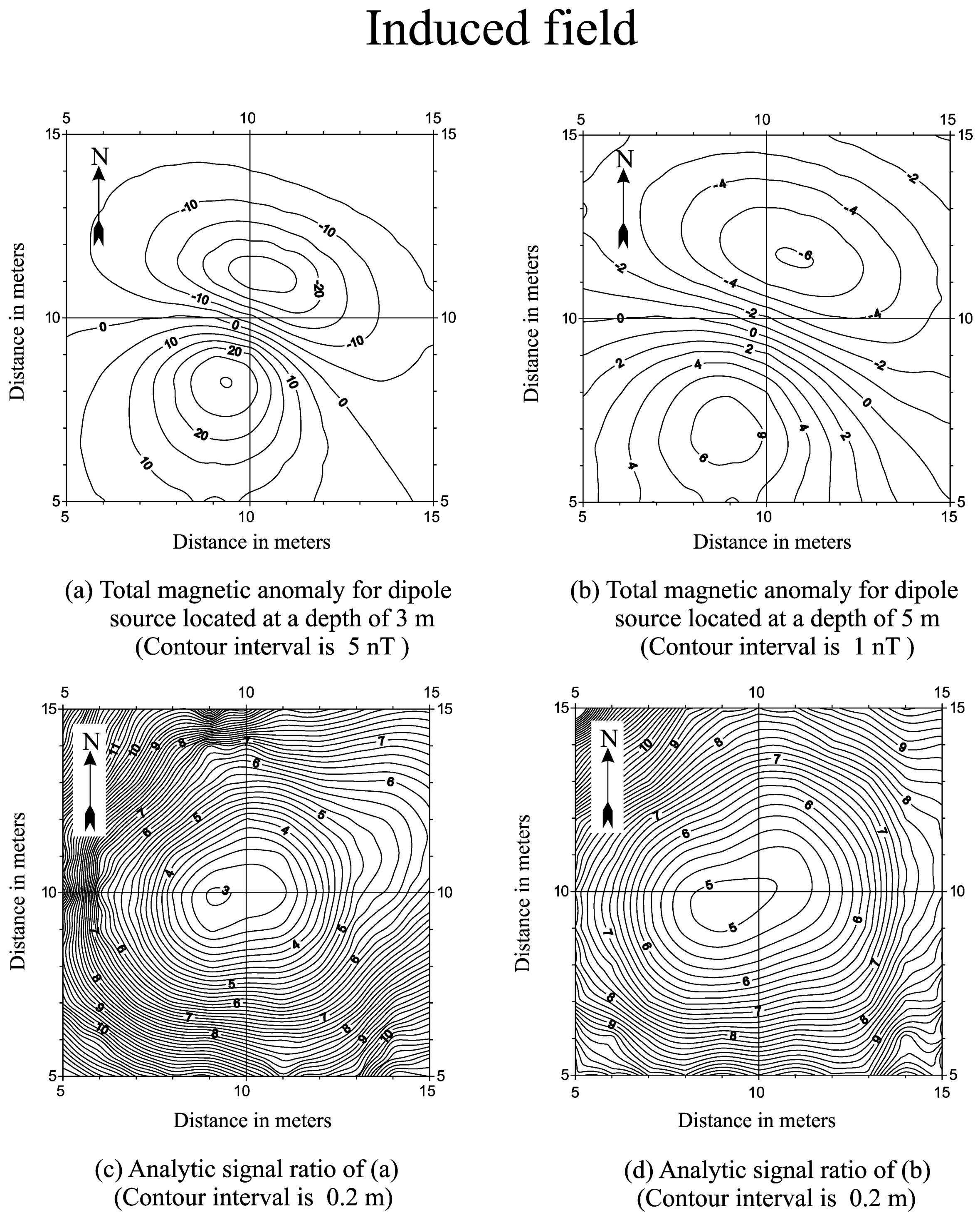

Fig. 3. Theoretical example of induced dipole sources placed at depths of 3 and 5 m: (a) and (b) are the total field anomaly maps of the two dipoles; (c) and (d) are the analytic signal ratios of their magnetic signatures (N is the geographic north; see the text for other parameters).

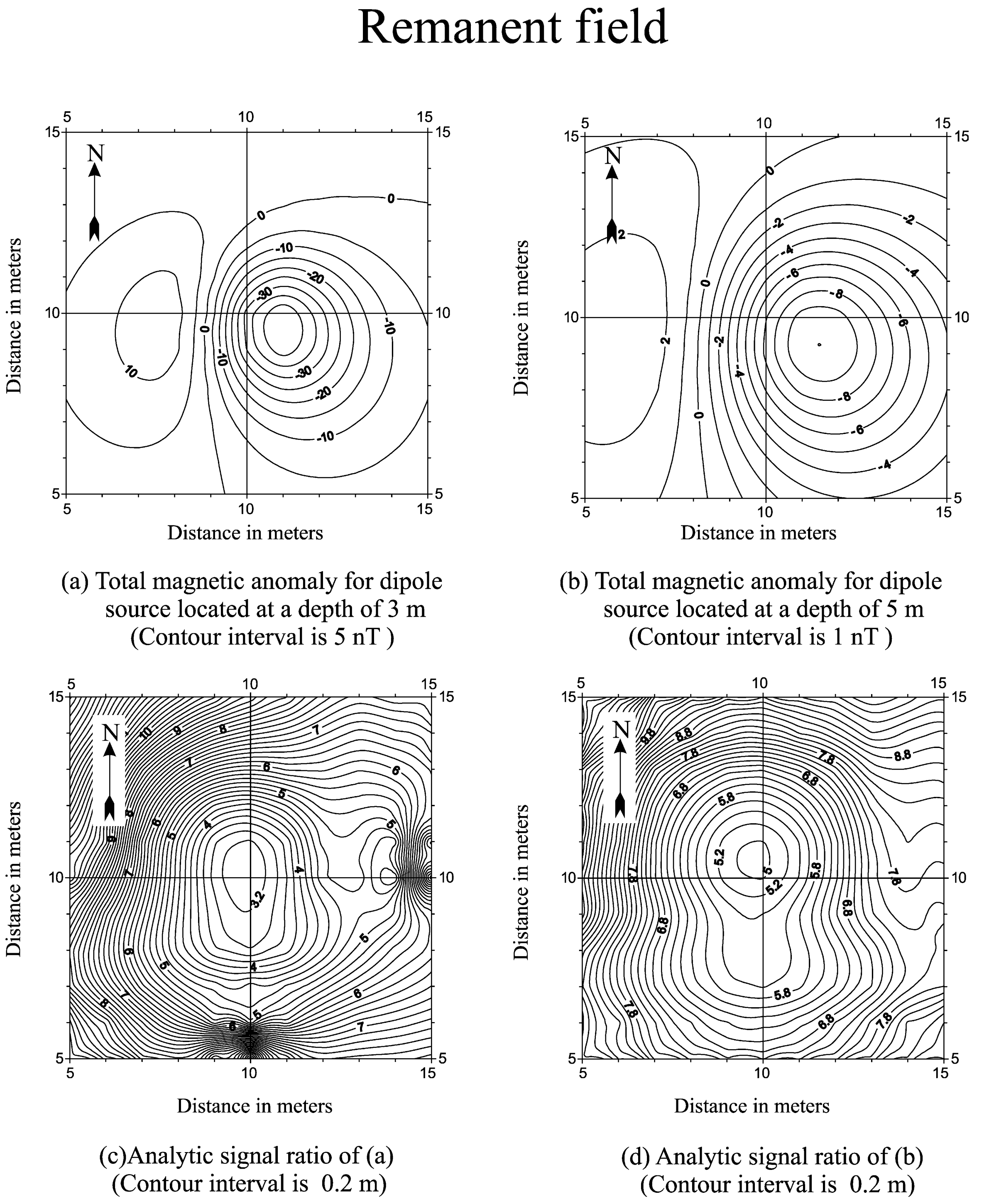

Fig. 4. Theoretical example of remanent dipole sources placed at depths of 3 and 5 m: (a) and (b) are the total field anomaly maps of the two dipoles; (c) and (d) are the analytic signal ratios of their magnetic signatures (N is the geographic north; see the text for other parameters).

In practice, the magnetic signature of ferrometallic objects can usually be broken into three contributions: the remanent magnetization, induced magnetization, and demagnetization effects. With the presence of remanent magnetization, the resultant magnetization direction will not be in the same direction as the induced magnetic field. To investigate the effect of remanent magnetization on the depth estimate using the analytic signal ratio, we tested the method with two examples of remanent dipole fields. In both these examples, the remanent direction consists of -30° of inclination and 90° of declination. We assumed that the remanent field of these sources is measured in an ambient (induced) magnetic field with an inclination of 60° and a declination of 0°. The remaining parameters (the location and magnetic moment) are the same as the induced examples in Fig. 3.

Fig. 4a,b shows the total field magnetic anomaly maps over the two sources. Similar to the examples described above, the ratios of the analytic signal signatures multiplied by factor 4 were calculated and are illustrated in Fig. 4c,d. The estimated depths at the horizontal locations of the dipole sources are 3.04 and 4.98 m, respectively. This means that the estimated depths are independent of the magnetization direction of either induced or remanently magnetic sources.

4. The field example

We show the feasibility of the depth estimation method formulated in this study for compact magnetic sources using field data over buried steel drums. The EG&G Geometrics Stanford University test site in California hosts a collection of environmental ferrometallic objects including sheets, pipes, and steel drums. The steel drums at the Stanford site are standard 55-gal drums buried at various depths and differ-

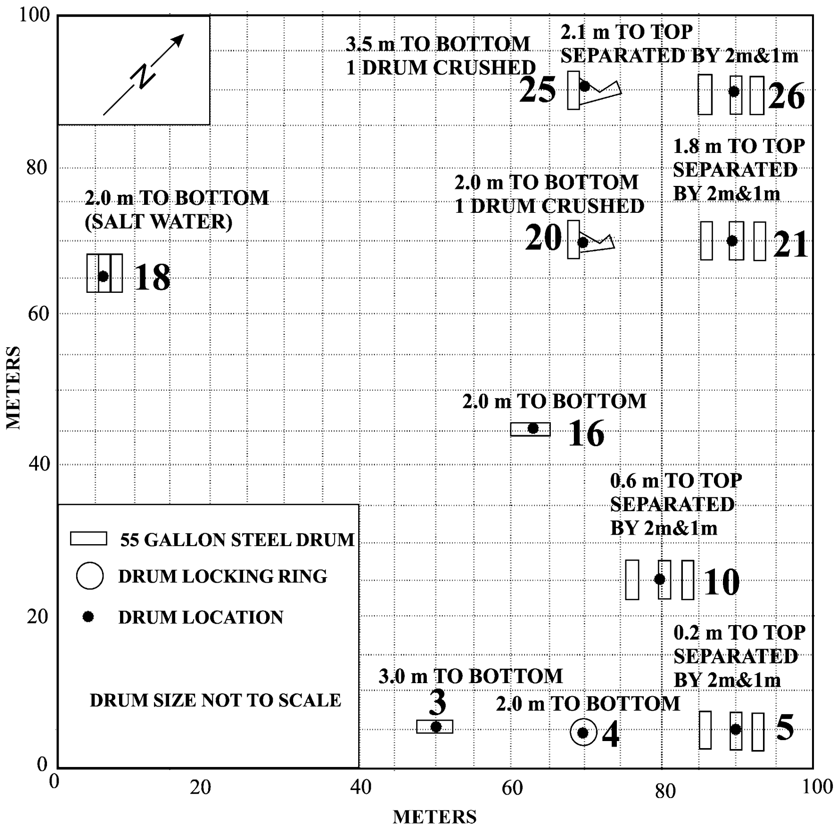

Fig. 5. Steel drums from the Stanford test site.

ent configurations (Fig. 5). The diameter of the drums is 0.59 m and the height is 0.98 m. The magnetic observations were taken over a set of traverses directed N45°W with a line spacing of 2 m and using a sampling rate of 0.3048 m (1 ft). The data were collected with a cesium vapor magnetometer model G858 with a sensitivity of 0.01 nT; the sensor was extended about 1 m in front of the operator and about 0.9 m above the ground surface. A base station magnetometer was used to observe and correct the diurnal magnetic variations. Fig. 6 shows the total field magnetic map of the Stanford test site.

To calculate the analytic signal signatures of the field data at the Stanford test site, the total field magnetic data (Fig. 6) were resampled into a regular grid with an interval of 0.5 m in both x and y directions.

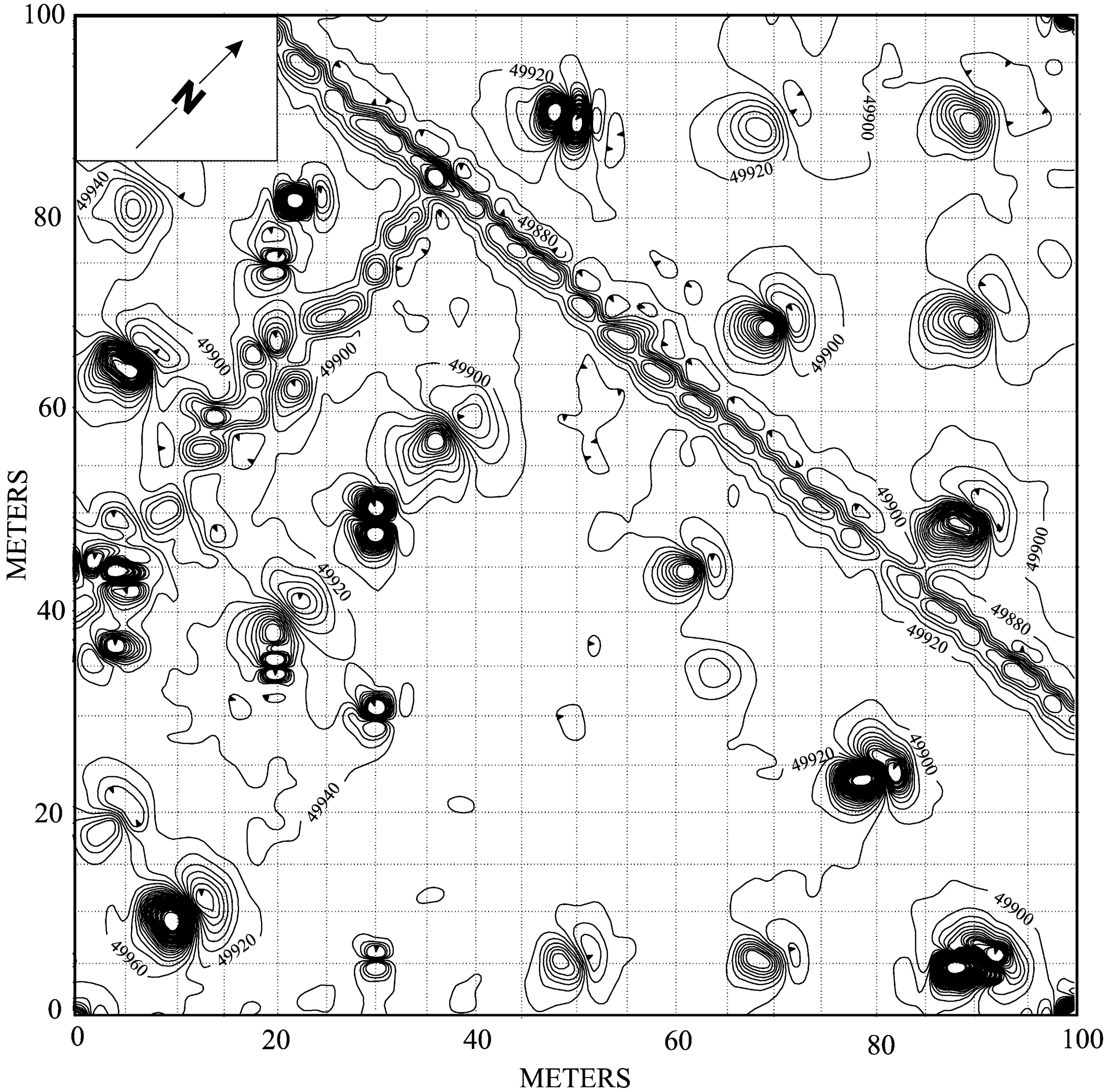

Fig. 6. Total field magnetic anomaly map of the Stanford test site (contour interval is 20 nT).

From this grid, appropriate derivatives were calculated using a Fast Fourier Transform (FFT) technique, from which the appropriate analytic signals were computed. Figs. 7 and 8 show maps of the AAS_0 and AAS_1 of the magnetic data at the Stanford test site. It can be seen that the maps reflect the existence of the magnetic objects. Generally, AAS maps better represent the locations of the shallow magnetic anomalies than total field magnetic maps because computation of the analytic signal depends on the gradients of the magnetic field, which implicitly enhance the magnetic response of shallow magnetic sources. Moreover, the values of the AAS are all positive, and they are more centered over their sources than the total field anomalies, leading to an easier interpretation of their approximate horizontal locations. However, noise is enhanced dur-

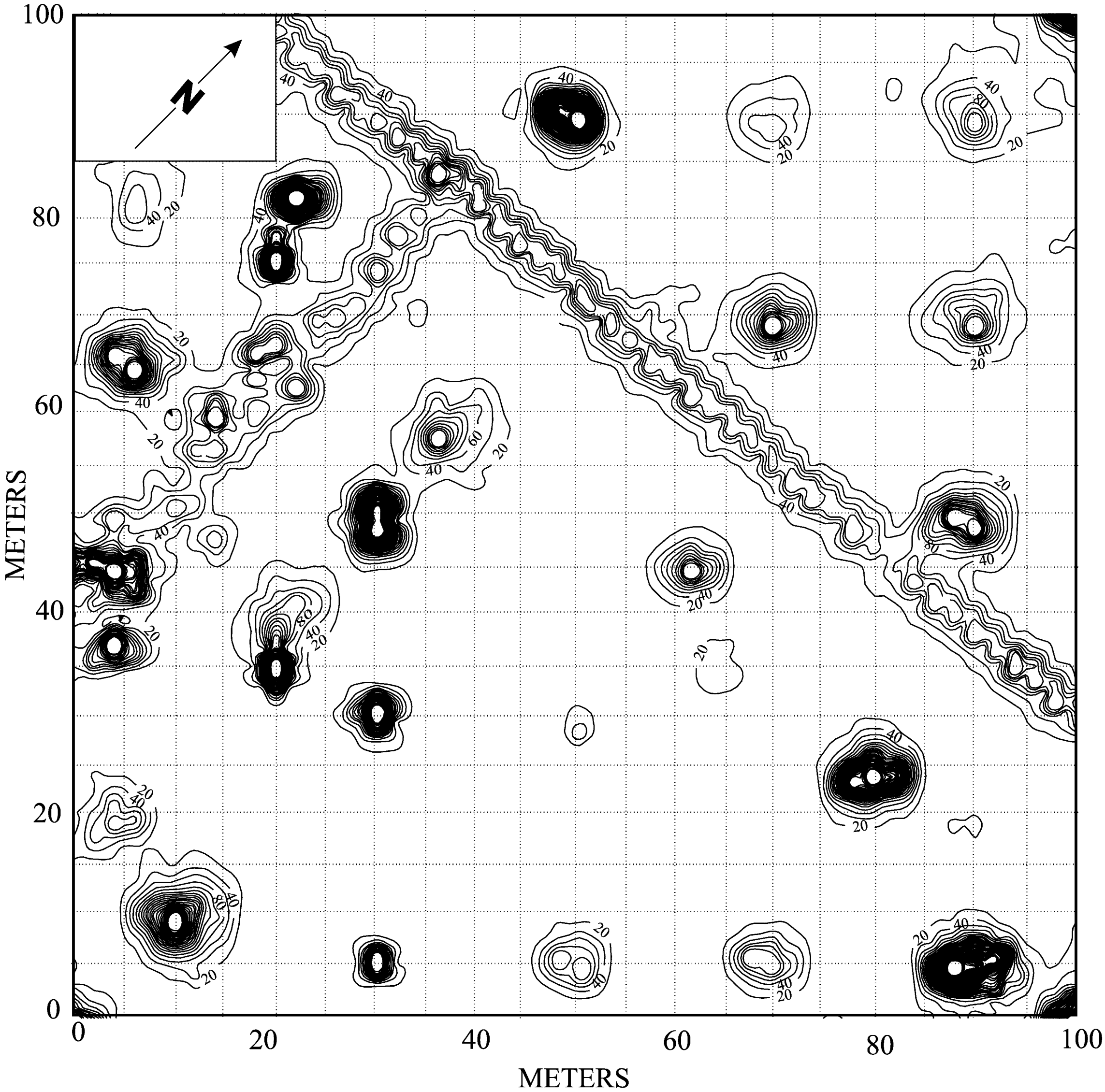

Fig. 7. The amplitude of the analytic signal of the total field magnetic anomalies of the Stanford test site (contour interval is 20 nT/m).

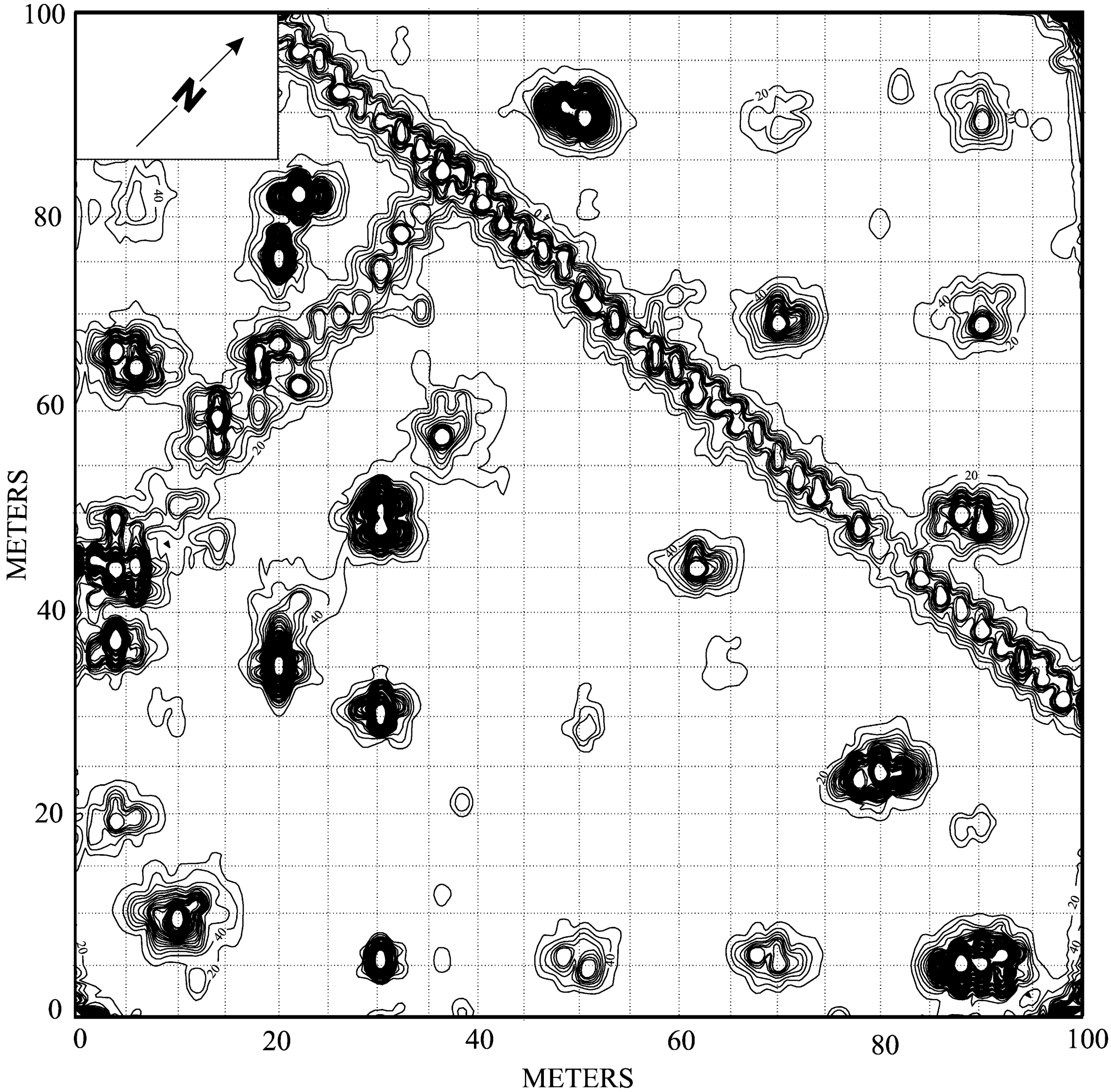

Fig. 8. The amplitude of the analytic signal map of the first vertical derivative of the total field magnetic anomalies of the Stanford test site (contour interval is 20 nT/m^2).

ing the calculation of the AAS and may lead to errors in the estimated depths using our method. A common approach is to use upward continuation (Roest et al., 1992) to reduce effect of such noise.

To estimate the depths of the buried steel drums at the Stanford test site using our AAS ratio method, we first located the values of the maxima of the AAS_0 using the procedure given by Blakely and Simpson (1986) and modified slightly by Roest et al. (1992). In this method, a linearity index is determined to describe the nature of detected maxima (e.g., index 1 for linear anomalies and index 4 for circular anomalies). For dipolar magnetic anomalies, an index of 4 would be useful because these anomalies, in most cases, are circular and have a very local extension. We used a threshold value of 20 nT/m (to minimize artifacts from noise) and an index of 4 to classify certain maxima as dipolar targets. Generally, the signal-to-noise ratio of magnetic anomalies of the steel drums at the Stanford test site is very high.

Fig. 9 shows the locations of 3D magnetic objects based on the AAS_0 response of the magnetic data at the Stanford site. The maxima of the AAS_0 are found above most of the drums. This may suggest that the induced magnetization dominates in these drums (the induced inclination at the test site is 62°) and/or the remanent magnetization, if present, has an inclination similar or greater than the induced inclination. The maximum of the AAS_0 response for the buried steel drums varies from about 80 nT/m for drums (25) to more than 2084 nT/m for drums (5). The maximum value of the AAS_0 is strongly dependent on the source-to-observation distance. Shallower sources such as drums (5) and (10) show significantly higher values of the maximum of the AAS_0. The depths of these drums are very shallow (1.4 and 1.8 m, respectively). Also, shallow single drums such as (3), (4), and (16) show values greater than those for anomalies produced by more than multiple drums such as (25).

Depth estimates based on our method (Table 1) show values close to the actual depths of the buried steel drums. Only for drum (3), the error in the estimated depth is 1.18 m. For other drums, the errors in the calculated depths are less than 0.6 m. These results show that the analytic signal approach can provide useful source locations for shallow environmental magnetic sources. However, horizontal locations based on the maximum values of the AAS must be verified using other techniques. Ravat (1996) pointed out that the Euler method usually gives accurate horizontal locations. Therefore, the Euler method can perhaps be incorporated with the above

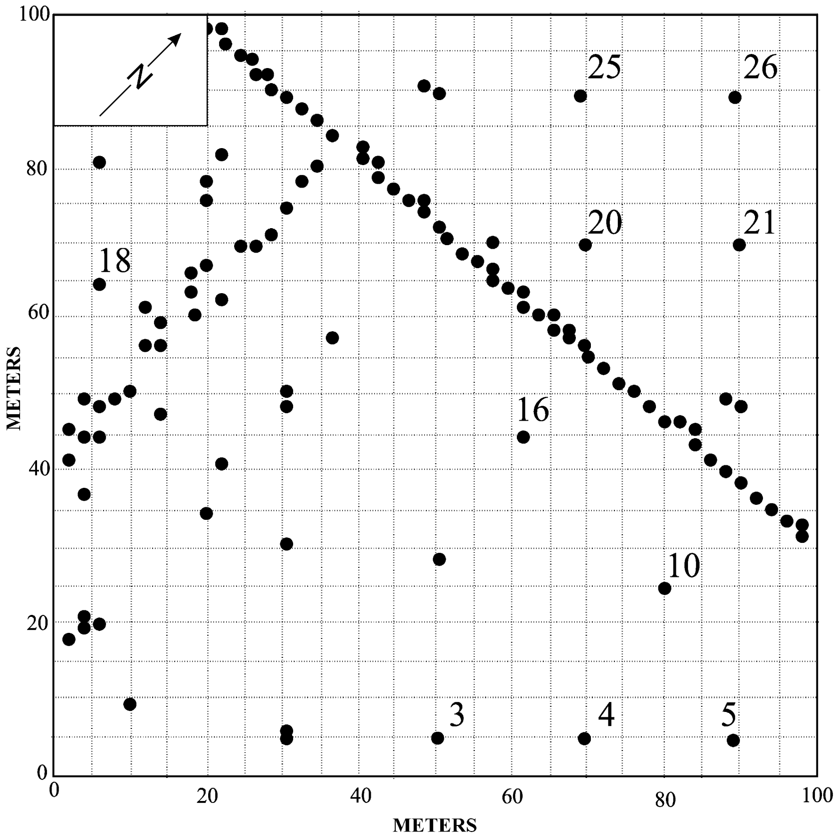

Fig. 9. The horizontal locations of the buried objects at the Stanford test site based on the maximum amplitude of the analytic signal.

Table 1
Result from the data at the Stanford test site

Drums	Actual depth[a] (m)	Maximum analytic signal response		Depth (m) based on the analytic signal ratios, $z=4AAS_0/AAS_1$
		AAS_0 (nT/m)	AAS_1 (nT/m^2)	
3[b]	3.6	126.32	208.38	2.42
4[b]	2.4	159.63	238.50	2.67
5	1.4	2084.11	4244.43	1.96
10	1.8	826.36	1454.13	2.27
16[b]	2.6	295.37	518.85	2.27
18	2.6	524.47	862.65	2.43
20	2.6	358.88	562.81	2.55
21	3.0	271.39	421.04	2.57
25	4.1	80.98	91.49	3.54
26	3.3	181.73	251.25	2.89

[a] Depth calculated from the elevation of the sensor to the mid-point of the drums.
[b] Anomaly produced by a single drum.

analytic signal approach to give reliable estimates of the source location even for a group of environmental magnetic objects.

5. Summary and conclusions

In this paper, we have analyzed the analytic signal approach of the total field magnetic anomalies and its applicability to compact magnetic objects in environmental magnetic investigations. Specifically, we have defined the analytic signal equation for induced magnetic dipoles. The equation indicates that the shape of the amplitude of the analytic signal (AAS) above dipolar sources is dependent on the value of the magnetic inclination. Accordingly, the maximum value of the AAS for a dipolar source does not always locate the source precisely. Maximum error in the horizontal location occurs at magnetic inclination of 30°. These shifts are also a function of the source-to-observation distance (up to 30% of the distance). Although these shifts are small for shallow environmental objects, care should be taken when interpreting dipole-like sources from aeromagnetic and satellite altitude magnetic data with the analytic signal approach. We have also developed a method to estimate depths of compact magnetic sources based on the ratio of the AAS of the magnetic anomaly to the AAS of the vertical gradient of the magnetic anomaly. The method provides a good estimate of the depths of compact magnetic sources regardless of their magnetization direction or the existence of remanence. Therefore, we can conclude that our new method is useful in estimating depths of compact magnetic objects in environmental investigations. We anticipate that the method will also be useful in deriving depths to equi-dimensional magnetic ore bodies and crustal intrusions, as long as data quality and spacing are adequate.

Acknowledgements

The authors greatly appreciate constructive and thoughtful comments of Prof. Domenico Patella, Dr. Jeffrey Phillips, and the Editor Dr. Niels Christensen. The authors thank EG&G Geometrics for providing the magnetic data. We extend our thanks to Dr. Mark Pilkington, Geological Survey of Canada, for providing a program for locating the maxima of a field. We are indebted to all of the staff of the Exploration Geophysics Laboratory of Kyushu University for their contribution and support during this work. The authors are also indebted to Dr. William D. Doll, Oak Ridge National Laboratory, for his comments on this work.

References

Atchuta Rao, D., Ram Babu, H.V., Sanker Narayan, P.V., 1981. Interpretation of magnetic anomalies due to dikes: the complex gradient method. Geophysics 46, 1572–1578.

Blakely, R.J., 1995. Potential Theory in Gravity and Magnetic Applications. Cambridge Univ. Press.

Blakely, R.J., Simpson, R.W., 1986. Approximating edges of source bodies from magnetic and gravity anomalies. Geophysics 51, 1494–1498.

Debeglia, N., Corpel, J., 1997. Automatic 3-D interpretation of potential field data using analytic signal derivatives. Geophysics 62, 87–96.

Gamey, T.J., Mahler, R., 1999. A comparison of towed and mounted helicopter magnetometer systems for UXO detection. Proceedings of Symposium on the Application of Geophysics to Engineering and Environmental Problems (SAGEEP1999), 783–792.

Gamey, T.J., Holladay, J.S., Mahler, R., 1997. Airborne measured analytic signal for UXO detection. Proceedings of Symposium on the Application of Geophysics to Engineering and Environmental Problems (SAGEEP1997), 853–862.

Gamey, T.J., Doll, W.E., Bell, D.T., 2000. Airborne UXO detection technology demonstration. Proceeding of Symposium on the

Application of Geophysics to Engineering and Environmental Problems (SAGEEP2000), 57–66.

Hsu, S.K., Sibuet, J.C., Shyu, C.T., 1996. High-resolution detection of geologic boundaries from potential anomalies: an enhanced analytic signal technique. Geophysics 61, 373–386.

Hsu, S.K., Coppens, D., Shyu, C.T., 1998. Depth to magnetic source using the generalized analytic signal. Geophysics 63, 1947–1957.

Linping, H., Zhining, G., Changli, Y., 1997. Comment on: 'An analytic signal approach to the interpretation of total field magnetic anomalies' by Shuang Qin. Geophysical Prospecting 45, 879–881.

MacLeod, I.N., Jones, K., Dai, T.F., 1993. 3-D analytic signal in the interpretation of total magnetic field data at low magnetic latitudes. Exploration Geophysics 24, 679–688.

Nabighian, M.N., 1972. The analytic signal of two-dimensional magnetic bodies with polygonal cross-section; its properties and use for automated anomaly interpretation. Geophysics 37, 507–517.

Nabighian, M.N., 1974. Additional comments on the analytic signal of two-dimensional magnetic bodies with polygonal cross-section. Geophysics 39, 85–92.

Nabighian, M.N., 1984. Toward a three-dimensional automatic interpretation of potential-field data via generalized Hilbert transforms: fundamental relations. Geophysics 49, 780–786.

Nelson, J.B., 1988. Comparison of gradient analysis techniques for two-dimensional magnetic sources. Geophysics 53, 1088–1095.

Pawlowski, J., Lewis, R., Dobush, T.D., Valleau, N., 1995. An integrated approach for measuring and processing geophysical data for the detection of Unexploded Ordnance. Proceedings of Symposium on the Application of Geophysics to Engineering and Environmental Problems (SAGEEP1995), 965–974.

Pederson, L.B., 1989. Relations between horizontal and vertical gradients of potential fields. Geophysics 46, 1572–1578.

Qin, S., 1994. An analytic signal approach to the interpretation of total field magnetic anomalies. Geophysical Prospecting 42, 665–675.

Ravat, D., 1996. Analysis of the Euler method and its applicability in environmental magnetic investigations. Journal of Environmental Engineering Geophysics 1, 229–238.

Roest, W.R., Verhoef, J., Pilkington, M., 1992. Magnetic interpretation using 3-D analytic signal. Geophysics 57, 116–125.

Thurston, J.B., Smith, R.S., 1997. Automatic conversion of magnetic data to depth, dip, susceptibility contrast using the SPITM method. Geophysics 62, 807–813.